**Atherosclerotic carotid plaque composition: a 3T and 7T MRI-histology correlation study**

MR Lopez Gonzalez (PhD)[a], SY Foo (MBChB)[b], WM Holmes (PhD)[c], W Stewart (MBChB,PhD)[d], KW Muir (MD, FRCP)[e], B Condon (PhD)[f], G Welch (MD)[g] and KP Forbes (PhD)[f]

[a]*Department of Clinical Physics and Bioengineering, Glasgow Royal Infirmary, Glasgow, UK.*

[b]*ST1, West of Scotland Radiology Training Scheme, NHS, Glasgow, UK.*

[c]*Glasgow Experimental MRI Centre, Institute of Neuroscience and Psychology, University of Glasgow, UK.*

[d]*Department of Neuropathology, Laboratory Medicine Building, Queen Elizabeth University Hospital, Glasgow, UK.*

[e]*Centre for Stroke and Brain Imaging Research, Institute of Neuroscience and Psychology, University of Glasgow, UK.*

[f]*Institute of Neurological Sciences, Queen Elizabeth University Hospital, UK.*

[g]*Vascular Surgery, Queen Elizabeth University Hospital, Glasgow, UK.*

Keywords: Atherosclerosis; stroke; Transient Ischeamia (TIA); Endarterectomy; Carotid; Magnetic Resonance Imaging

Abstract

Background and Purpose

Carotid artery atherosclerotic plaque composition may influence plaque stability and risk of thromboembolic events, and non-invasive plaque imaging may therefore permit risk stratification for clinical management. Plaque composition was compared using non-invasive in-vivo (3T) and ex-vivo (7T) MRI and histopathological examination.

Methods

Thirty three endarterectomy cross sections, from 13 patients, were studied. The datasets consisted of in-vivo 3T MRI, ex-vivo 7T MRI and histopathology. Semi-automated segmentation methods were used to measure areas of different plaque components. Bland-Altman plots and mean difference with 95% confidence interval were carried out.

Results

There was general quantitative agreement between areas derived from semi-automated segmentation of MRI data and histology measurements. The mean differences and 95% confidence bounds in the relative to total plaque area between 3T versus Histology were: fibrous tissue 4.99 % (-4.56 to 14.56), lipid-rich/necrotic core (LR/NC) with haemorrhage -1.81% (-14.11 to 10.48), LR/NC without haemorrhage -2.43% (-13.04 to 8.17), and calcification -3.18% (-11.55 to 5.18). The mean differences and 95% confidence bounds in the relative to total plaque area between 7T and histology were: fibrous tissue 3.17 % (-3.17 to 9.52), LR/NC with haemorrhage -0.55% (-9.06 to 7.95), LR/NC without haemorrhage -12.62% (-19.8 to -5.45), and calcification -2.43% (-9.97 to 4.73).

Conclusions

This study provides evidence that semi-automated segmentation of 3T/7T MRI techniques can help to determine atherosclerotic plaque composition. In particular, the high resolution of ex-vivo 7T data was able to highlight greater detail in the atherosclerotic plaque composition. High field MRI may therefore have advantages for in vivo carotid plaque MR imaging.

## Introduction

Stroke is the third leading cause of death and the single largest cause of adult disability in the UK[1]. Eighty-five percent of strokes are ischaemic, and up to 20% of these are caused by carotid atherosclerosis[2].

While carotid endarterectomy (CEA) reduces the risk of ipsilateral stroke in patients with moderate or severe stenosis, 70% of recently symptomatic patients with severe stenosis remain stroke-free over the next 5 years with medical therapy alone.[3] These surgical decisions were based on percentage luminal stenosis, leading several authors to suggest that luminal stenosis measurements alone cannot predict high-risk atherosclerotic carotid plaques. Further, morphological features, such as plaque ulceration and inflammation, are now recognised to be important independent risk factors for embolic stroke.[4-5] It has been suggested that the stratification of carotid plaque should combine cerebral hemodynamic and plaque composition assessments additional to luminal stenosis.[6-7] Unnecessary surgery could be avoided among those with low risk of events by targeting treatment at high-risk subgroups and not simply relying on the degree of stenosis.[8]

Pathologically, it is possible to identify features of atherosclerotic plaques that are predisposed to embolism and subsequent stroke, such as haemorrhage, ulceration of the fibrous cap, or a large lipid core.[9-10] Magnetic resonance imaging (MRI) is a promising imaging modality for carotid plaque visualisation.[11-17] In addition, high magnetic field strengths offer improved resolution and the potential to detail plaque substructure beyond routine field strengths. Carotid plaque MR imaging (CPI) using a multi-contrast approach, potentially allows differentiation between the major atheromatous components, namely haemorrhage, lipid, and fibrous tissue. The technique uses an algorithm, which allows separation of the atheromatous components, based on their signal intensities under different MR weightings. Some reports have also suggested that CPI can offer additional structural information, for example on the integrity of the atheromatous fibrous cap. [13-15] Such imaging

biomarkers could allow differentiation of active atheromatous plaques, which carry a higher risk of embolic stroke, from indolent atheromatous plaques. Risk stratification of patients with carotid stenosis and recent stroke or TIA may permit clinicians to select only those patients at highest risk for endarterectomy procedures.

Most CPI has been performed at 1.5T, although a few recent studies have used 3T. Similar relative appearances on multi-contrast techniques[18-21] have been report at 1.5T and 3T. Some studies have compared plaque composition in vivo qualitatively, as defined by MRI, to the pathologic appearances post-carotid endarterectomy, thus validating imaging findings at 3T.[22] Ex-vivo imaging to date has been limited to studies at 1.5T.[10,14-15,23-31]

The aim of this study was to (1) perform in-vivo and then ex-vivo imaging on the same atheromatous plaque, with comparison to histopathology (2) define an algorithm allowing differentiation of plaque components at 7T and (3) assess whether 7T offers potential additional utility in defining plaque composition over lower field strengths.

## Material and Methods

### Patient population

The study was undertaken following ethical approval and with written informed consent. Subjects were drawn from a group of 30 patients with minor acute (within prior month) cerebral ischaemic symptoms, with corresponding >50% carotid stenosis or plaque ulceration (mean age: 71.5±15.5 years, and female/male ratio of 13/17) on CT Angiography. The exclusion criterion was any contra-indication to MRI.

24 subjects underwent 3T MR Imaging; 13 subjects were included in this study having completed CEA, 3T in-vivo and 7T ex-vivo MRI of the CEA specimen.

**Imaging technique, specimen preparation and histology**

(1) In-vivo 3T MRI

Imaging was performed with a 3T MRI GE Signa Excite HD and a 4–channel surface coil (Herman Flick). The protocol included: 2D & 3D Time-of-Flight (TOF) MR angiogram (MRA) of carotid bifurcations (TR/TE/Flip Angle/Slice thickness: 16.52ms/3.848ms/80°/3mm, 89 slices). Carotid plaque imaging through the carotid bifurcation: axial 2D FSE (fast spin echo) double inversion recovery (DIR;TI: 1550ms, fat sat), peripheral cardiac gating: T1-W (TR/TE:722-1034ms/7-12ms), PD-W (TR/TE:1411-2857ms/8-21ms) & T2-W (TR/TE:1237-2105ms/57-62ms, depending on heart rate) ±T1-W post gadolinium (n=12/16): 3-5 slices (2-2.5mm), NEX=1, matrix 512 x512x8/FOV: 14x14x1.25 $cm^3$. Resolution: 273x273x2500 $\mu m^3$, scan time ~ 30 minutes.

(2) Specimen preparation and ex-vivo 7T MRI

CEA specimens were immediately fixed following surgical removal in 10% formaldehyde. They were rehydrated in sterile phosphate buffered saline (PBS), at room temperature for 24 hours prior to scanning and then placed in a de-gassed Fomblin-filled syringe along with a phantom (1g/l $MgCl_2$) for imaging. The MRI system used was a 7T Bruker Biospin Biospec 70/30 MRI (microimaging gradient insert (model BG-6), 100-A gradient amplifiers (1,000mT/m), 35mm Bruker birdcage). The protocol included: T1-W FLASH (TR/TE/flip angle:40ms/2.315ms/30°/matrix: 280x170x170/FOV: 2.8x1.7x1.7$cm^3$/ NEX:20), T2-W multi slice multi echo (MSME) (TR/TE:1200ms/8.02ms/matrix 155x94x94/ FOV:2.8x1.7x1.7$cm^3$/ NEX:6). Diffusion-weighted imaging: stimulated echo (TR/TE: 750ms/13ms, delta: 2.2 ms, b-values: 0 & 750 s/$mm^2$, along 3 directions. Resolution: 100$\mu m^3$, scan time ~38 hours per specimen.

(3) Histology

Following ex-vivo MR, the specimen was divided into approximately 5 sections, each embedded en bloc in paraffin wax. 4μm thick sections were taken from each section and stained with Haematoxylin & eosin (H&E) and Miller's Elastic/van Gieson (EVG).

**Analysis**

(1) Histology*:* H&E sections were digitised (Nanozoomer RS Digitizer; Hamamatsu Photonics K.K.) and those showing a significant plaque burden were selected. The major plaque components of fibrous tissue, lipid-rich necrotic core (LR/NC), haemorrhage and calcification were delineated manually using Adobe Photoshop CS3 (drawing tablet: Trust 16485; Trust International B.V.)

(2) Matching of imaging and histology: The digitized histological images were co-registered to the ex-vivo MR images using the Analyze (AnalyzeDirect, Inc.) linear registration method. These were then visually matched to the closest 3T slice. For ex-vivo MR, 58 sections from 11 plaques were successfully matched to histology, with 33 sections then co-registered with in-vivo 3T MR.

(3) In vivo MRI Carotid plaque segmentation based on multi-contrast signal intensity relative to the sternocleidomastoid muscle, was carried out using a semi-automatic method developed in MatLab and Image J, using the criteria reported by Saam et al.[15] Image J was used to individually select the sternocleidomastoid muscle using the threshold tool defining the iso-intense image intensities, any tissue under this range was considered hypointense or above hyperintense. These threshold values were used in Matlab. The images were first segmented into hypo, iso and hyper intense compartments and Sam's criterion was used with conditional statements in Matlab.

(4) Derivation of predictive model of multi-contrast 7T MRI for classification of plaque components: The aim was to develop a predictive model for ex-vivo 7T MRI to allow classification of plaque components, based on the varied signal intensities of components, on different image-weightings. Regions of interest (ROI) were drawn around classic examples of the major plaque components on histology, derived from 9

specimens as derivation data set (Table 1). The MRI signal intensities of the derivation data set were then used to define the areas of each plaque component, using an in-house semi-automated programme in MATLAB (MatLabWorks, Natick, USA).

(5) Once the images were segmented the area for each individual plaque component of interest was determined using Image J (http://rsb.info.nih.gov/ij/). All the corresponding MRI (in-vivo and ex-vivo) and digitised histology slices were then compared.

Table 1. Tissue Classification Scheme for 7T MR images. This table was constructed based on the different MR signal intensities of the plaque components according to the training dataset. The numbers represent the mean relative signal intensities ± 0.5 SD.

**Statistical Analyses**

All statistical analyses were performed using Prism 5. All data are expressed as mean ± SD. Area measurements are expressed in $cm^2$. The overall agreement between area measurements of the 4 plaque components by histology and MRI was assessed using Bland-Altmananalysis which plots difference in area measurements (MRI-Histology) against average area measurements.[32] We considered each artery as a sample in order to lessen the impact of mismatch between histology and MRI for possible statistical dependence of multiple locations per artery. Paired t test was performed to compare the plaque composition as percentage of the total vessel wall between MRI (in-vivo and ex-vivo) and Histology. Pearson correlation calculations were carried out using Excel to assess shrinkage of the different carotid plaque components.

## Results

Data were collected from twenty-four subjects but only 13 subjects completed in-vivo 3T MRI as well as ex-vivo 7T MRI and histologic assessment of the carotid endarterectomy specimen. Two further patients were excluded as direct coregistration of histopathology and 3T MR images was not possible. The demographics of this subgroup were, mean age: 65.2±6.6 years, and female: male ratio of 1:10. Subjects all presented with acute cerebral ischaemia (stroke:4;TIA:7), within the 4 weeks before MRI scanning (mean 10.4±8.4 days). Subjects had a range of risk factors for stroke: Smoker:9, hypertension:8. hypercholesterolemia:9; diabetes mellitus:2. The mean interval from 3T imaging to surgery was 3.9(SD 3) days.

Direct comparison of MRI (in-vivo 3T and ex-vivo 7T) and histology for 11 patients was carried out, examples are shown in figures 1 and 2. Results are summarised below and tabulated in figure 3.

*Figure 1. MR multicontrast weighted images of vulnerable plaque were obtained at 7T ex vivo (A-C) and at 3T in vivo (E-H). Histological images stained with haematoxylin & eosin digitised in D. A and E: T1-w, B and F: T2-w, C: DWI, H: PD-w.*

*Figure 2. Segmentation of the 7T (left), Histology (middle) and 3T (right) MR images. 7T MR images were segmented using the phantom normalised signal intensity and the criterion described in table 1. 3T MR images were segmented using Saam's criterion[15] with signal intensities relative to the sternocleidomastoid muscle. Histology sections were segmented manually. Orange/Yellow = Fibrous tissue, Green = LR/NC with haemorrhage and blue = LR/NC without haemorrhage.*

*Figure 3. Plaque composition in percentage of total plaque area of the 3T MRI, 7T MRI and the histology dataset, per artery.*

## 3T MRI In-vivo vs. Histology

The mean total plaque area was greater on MRI than histology (mean difference 8.59 $cm^2$ (8.21 to 8.97 95% CI)). This is an expected finding due to plaque shrinkage during fixation and histological processing. The areas of plaque subcomponents were corrected for this, by defining relative to total plaque area (percentage of total plaque area) and reported in table 2.

Table 2. Areas of plaque components in $cm^2$ and corresponding percentage areas of histology, in-vivo 3T MRI and ex-vivo 7T MRI measurements. Including the paired t test P-values of the corrected percentage areas.

Bland-Altman analysis (figures 3) suggests that areas of fibrous tissue are overestimated by in-vivo 3T MRI compared with histology (3a). The mean difference and 95% confidence bounds for fibrous tissue were 0.59 (0.08 -1.09), in the case of LR/NC w Haem (with Haemorrhage) 0.15 (-0.27 – 0.58), LR/NC wo Haem (without Haemorrhage) 0.11 (-0.38 – 0.59) and calcification 0.038 (-0.159 – 0.237). The mean differences and 95% confidence bounds in the relative to total plaque area are: fibrous tissue 4.99 (-4.56 to 14.56), LR/NC w Heam -1.81 (-14.11 to 10.48), LR/NC wo Heam -2.43 (-13.04 to 8.17), and calcification -3.18 (-11.55 to 5.18).

*Figure 4. Bland-Altman plots for the different plaque components of Histology and in-vivo 3T MRI in $cm^2$. These results show a consistent overestimation of the plaque components using 3T MRI.*

Correlation analysis

The strongest correlation between in-vivo 3T MRI and histological area measurements was for LR/NC with Haemorrhage ($r = 0.78$, $p = 0.005$), and calcification ($r = 0.74$, $p = 0.009$). A fair correlation was found for LR/NC without Haemorrhage ($r = 0.66$, $p = 0.027$) and fibrous tissue ($r = 0.66$, $p = 0.042$) and a poor correlation was found for haemorrhage ($r = 0.26$, $p = 0.437$).

Plaque composition

Plaque composition calculated as percentage of the vessel wall was comparable for 3T MRI and histology for the calcification (7.9% vs 11.08%; P=0.17), LR/NC w Haem (21.45% vs 23.26%; P=0.86), fibrous tissue (70.64% vs 65.65%; P=0.32) and LR/NC wo haem (15.78% vs 18.22%; P=0.45).

## 7T MRI Ex-vivo vs. Histology

The mean total plaque area was again greater on ex-vivo 7T MRI than histology (2.75 $cm^2$ (2.42 to 3.07 95% CI), an expected finding due to plaque shrinkage during fixation and histological processing. The plaque subcomponents were corrected for this, by defining relative to total plaque area as in the in-vivo results, table 2. The corrected area of plaque components between histology and MRI did not differ significantly for most components, but there was a significant difference for LR/NC wo heam and haemorrhage.

The Bland-Altman plots (figure 5) show good agreement for area measurements of lipid rich necrotic core (LR/NC) with or without haemorrhage, and calcification. MRI slightly overestimated regions of fibrous tissue. The mean difference in fibrous tissue and 95% confidence bounds were 0.19 (-0.203 - 0.593) in the case of LR/NC w Heam 0.053 (-0.108 – 0.213), LR/NC wo Heam -0.078 (-0.34 – 0.18) and calcification 0.002 (-0.187 – 0.192). The mean differences and 95% confidence bounds in the relative to total plaque area are: fibrous tissue 3.17 % (-3.17 to 9.52), LR/NC w Heam -0.55 (-9.06 to 7.95), LR/NC wo Heam -12.62 (-19.8 to -5.45), and calcification -2.43 (-9.97 to 4.73).

*Figure 5. Bland-Altman plots for different plaque components of Histology and ex-vivo 7T MRI in $cm^2$. These results show a consistently overestimation of the plaque components using 7T MRI.*

Correlation Analysis

There was fairly strong correlation between MRI and histology area measurements of LR/NC with haemorrhage (*r* = 0.84; p = 0.001) and fibrous tissue (r = 0.75; p = 0.008). A fair correlation was for haemorrhage (r = 0.63; p = 0.039). The correlation between MRI and histologic area measurements for calcification (r = 0.4; p = 0.22) and LR/NC wo haem (*r* = 0.4; p = 0.23) were less good. For calcification there was poor correlation between histology and ex-vivo, however, absolute area and percentage area of the total calcification did not differ (histology: 0.88±0.1 $cm^2$ (11.08%), and MRI 0.9±0.04 $cm^2$ (8.46%), p = 0.945, (p = 0.69)), providing evidence that calcification was not or less affected by the fixation procedure.

Plaque composition

Plaque composition calculated as percentage of the total plaque area was comparable for 7T MRI and histology for the calcification (8.46% vs 11.08%; P=0.68), LR/NC w Haem (22.71% vs 23.26%; P=0.9), fibrous tissue (68.82% vs 65.65%; P=0.34) and LR/NC wo haem (5.58% vs 18.22%; P=0.01).

## *In-vivo* versus *ex-vivo*

An average difference of around 44.5±18.7% in area was found when comparing in-vivo 3T MRI measurements versus histopathology and 29.6±5% when comparing in-vivo 3T MRI and ex-vivo 7T MRI modalities. The average difference when comparing 7T MRI and histopathology was 16.1±16%.

## Discussion

We confirmed that in-vivo 3T MRI can determine the relative areas of components of carotid atherosclerotic plaque compared to subsequent histopathology analysis, as reported previously at 1.5 T.[15,23,27,33] Though Gao and colleagues[34] have reported a qualitative comparison of 3T MR and histology, we believe ours is the first study to report a quantitative comparison between 3T MR imaging with histopathology in human atherosclerotic carotid

plaques. In addition, this is the first study to simultaneously compare quantified high resolution ex-vivo 7T MRI with histopathology.

Stratification of high-risk atherosclerotic plaque has been reported in several papers, the consensus being that MRI carotid plaque composition may aid risk stratification and treatment selection in acute stroke and TIA. For example, the presence of intraplaque haemorrhage has been reported as strong predictor of cerebral events. [35] Fibrous cap rupture has been reported more prevalent in symptomatic patients compared with asymptomatic. Mixed results have been published regarding the association of intraplaque calcification and the stabilisation of carotid plaques. [36]

Our in-vivo clinical 3T MRI results consistently overestimated the areas of all plaque components when compared to histological sections, while pre-clinical ex-vivo 7T MRI also overestimates the areas but to a lesser degree. The main causes of overestimation of plaque components is specimen shrinkage due to the fixation procedure. Shrinkage of arterial rings specimens have been reported as 19-25% in area by Dobrin[37] using different fixation methods. In this reference it was confirmed that fixation and embedding can cause volume changes and may cause tissue distortion. Shrinkage of specimens size compared to MRI, has been reported to be on average 15% in width and 30% in length by Eubank 1998 and co-workers.[38]

The MRI in-vivo and ex-vivo overestimation has been reported before in a number of references.[23,39,40] We found an average higher overestimation in area when comparing in-vivo 3T MRI versus histology than comparing in-vivo versus ex-vivo MRI as expected. Yuan and co-workers[40] attributed in-vivo overestimation on MRI to the inclusion of the intimal lesion, media, and adventitia while the ex-vivo measurements included only the intimal lesion and part of the media. Additionally, in-vivo measurements have larger voxel size than ex-vivo measurements which results in an overestimation of the wall and boundaries between plaque

components, i.e. partial volume effects.[40] Moreover, with in-vivo MRI the delineation of the carotid artery with surrounding tissue was not clear, this is because FSE imaging techniques suffer from blurring caused by non-uniformity of the k-space sampling.[41]

Even after the plaque subcomponents were corrected for shrinkage due to fixation, by defining relative to total plaque area, ex-vivo results show discrepancies in haemorrhage and LR/NC without haemorrhage when compared to histopathology. Haemorrhage was overestimated and LC/NC without haemorrhage was underestimated. This discrepancy between histology and 7T MR in haemorrhage quantification could be explained by the MRI techniques used (T1-w, T2-w and DWI). Boekhorst and colleagues used a different protocol consisting of T1-w GE, T2-w FSE, PD-w FSE and IR-SE MRI techniques at 9.4T, and reported that the combination of these sequences improved the sensitivity to intra plaque haemorrhage compared to our (T1-w, T2-w and DWI) protocol. Haemorrhage as identified on histology may have distinct 3T and 7T properties that have been overlooked in this study, such as susceptibility effects. Moreover, we were unable to construct a threshold range for a subcategory for haemorrhage mainly due to the limited sample size of our study and the overall small percentage of fresh and recent haemorrhage in our samples. Another factor that could be relevant is the interval between in-vivo MR and surgery as haemorrhage evolves with time and may influence the MRI signal appearances.

In-vivo 3T MRI results show good agreement with most histological components in absolute areas ($cm^2$) and relative to total plaque area except for haemorrhage and LR/NC wo haem. This has been reported before and this mismatch results as boundaries of intra plaque haemorrhage are difficult to determine within the LR/NC areas.[15,31]

Saam et al.[15] reported that measurements of the mean area of calcification did not differ significantly between histology and in-vivo MRI, similar to our findings. They attributed their

findings to: i) calcification shrinkage being less that other components and ii) partial volume effects. Our results show that the fibrous tissue and LR/NC with haemorrhage have the largest degree of shrinkage due to specimen processing (~76 & 63%) compared with calcification (~39%). Comparison of our results at 3T, with previous work at 1.5T, [15] shows similar percentages for LR/NC without haemorrhage and total fibrous tissue, though our calcification measurements did not showed the underestimation reported by the authors.

An additional source of error may arise from partial volume effects, where an individual voxel contains two or more tissue types. In such cases the signal from the voxel is a weighted average of the component tissue types, which may lead to misclassification of plaque components from the averaging of the MRI signal over the whole voxel. This will be a bigger affect in the case of 3T MRI where the spatial resolution is lower compared with 7T and histology.

## Study Limitations

There are limitations to our study which must be noted.

While 7T clinical and pre-clinical MRI scanners offer increased spatial resolution and signal-to-noise ratio (SNR) that may be attractive for imaging of small structures like the carotid artery wall, the higher magnetic field causes tissue T1 relaxation times to be longer and T2 values shorter compared to lower field systems, increasing the scanning time and reducing some of the improvements in signal-to-noise from the high field, respectively. Motion at high magnetic field is a more severe problem as it has been reported that the object has to maintain position with accuracy 10 times higher than the resolution.[42] Our ex-vivo measurements were carried out in a 7T pre-clinical experimental setup, whereas in practice this protocol could not be replicated exactly at 7T or similar high field clinical scanner. Development of suitable in-vivo high field imaging methods represents a significant technical challenge. Finally, though 30 patients were originally recruited, not all received 3T, 7T and Histology analysis. Thus, in total there were 11 patients with all measures.

## Conclusions

This study demonstrated that 7T and 3T MR imaging modalities can reliably detect atherosclerotic plaque composition when compared with histopathology. Our study is the first to our knowledge to compare 7T and 3T MRI quantitatively with histopathology.

Development of clinical 7T MRI of artheroclerotic carotid arteries may improve identification of the morphological feature and composition of vulnerable plaques. On the other hand there are still limitations such as the increase in specific absorption rates and the inhomogeneity in transmit fields. Therefore the overall benefits of in-vivo 7T MRI still need to be demonstrated and comparison made with lower field strengths, considering not only scanning length, signal-to-noise, and contrast-to-noise rations, but also the extensive contraindications for patient scanning.

## Acknowledgments

MRLG received a travel grant from Guarantors of Brain UK, and IPEM Bursary Scheme to present this work at the 2009, and 2013 ISMRM conferences, respectively.

## Sources of Funding

This work was funded by the Chief Scientist Office, Scotland.

## Disclosures/conflict of interest

The authors declare no conflicts of interest.

## References

1. Department of Health - Reducing Brain Damage: Faster access to better stroke care. National Audit Office. 2005. Available at: www.nao.org.uk/report/department-of-health-reducing-brain-damage-faster-access-to-better-stroke-care/. Accessed January 15, 2013.
2. Markus H. Revascularization of Asymptomatic High-Grade Carotid Stenosis Is Still Indicated in Some Cases. Stroke 2011;42:1152-1153.
3. Hankey GJ. Stroke Treatment and Prevention: An evidence-based approach. Cambridge University Press. 2005:264.
4. Homburg PJ, Rozie S, van Gils MJ, et al. Association Between Carotid Artery Plaque Ulceration and Plaque Composition Evaluated With Multidetector CT Angiography. Stroke 2011;42:367-372.
5. Marnane M, Prendeville S, McDonnell C, et al. Plaque Inflammation and Unstable Morphology Are Associated With Early Stroke Recurrence in Symptomatic Carotid Stenosis. Stroke 2014;45:801-806.
6. Gupta A, Marshall RS. Moving Beyond Luminal Stenosis: Imaging Strategies for Stroke Prevention in Asymptomatic Carotid Stenosis. Cerebrovasc Dis 2015;39:253-261.
7. Lindsay AC, Biasiolli L, Lee JMS, et al. Features Associated With Increased Cerebral Infarction After Minor Stroke and TIA. Cardiovasc Imaging 2012; 5:388-396
8. Markus HS, King A, Shipley M, et al. Asymptomatic embolisation for prediction of stroke in the Asymptomatic Carotid Emboli Study (ACES): a prospective observational study. Lancet Neurol 2010;4422:70120-4.
9. Fayad ZA, Fuster V. Clinical imaging of the highrisk or vulnerable atherosclerotic plaque. Circ Res 2001;89:305–316.
10. Takaya N, Yuan C, Chu BC, et al. Association between carotid plaque characteristics and subsequent ischemic cerebrovascular events: a prospective assessment with MRI-initial results. Stroke 2006;37:818–823.

11. Toussaint JF, LaMuraglia GM, Southern JF, Fuster V, Kantor HL. Magnetic resonance images lipid, fibrous, calcified, hemorrhagic, and thrombotic components of human atherosclerosis in vivo. Circulation 1996;94:932–938.
12. Hatsukami TS, Ross R, Polissar NL, Yuan C. Visualization of fibrous cap thickness and rupture in human atherosclerotic carotid plaque in vivo with high-resolution magnetic resonance imaging. Circulation 2000;102:959–964.
13. Cai JM, Hatsukami TS, Ferguson MS, Small R, Polissar NL, Yuan C. Classification of human carotid atherosclerotic lesions with in vivo multicontrast magnetic resonance imaging. Circulation 2002;106:1368–1373.
14. Clarke SE, Hammond RR, Mitchell JR, Rutt BK. Quantitative assessment of carotid plaque composition using multicontrast MRI and registered histology. Magn Reson Med 2003;50:1199–1208.
15. Saam T, Ferguson MS, Yarnykh VL, Takaya N, et al. Quantitative Evaluation of Caritod Plaque Composition by In Vivo MRI. Arterioscler Tromb Vasc Biol 2005;25:234-239.
16. Wasserman BA, Wityk RJ, Trout HH, Virmani R. Low-grade carotid stenosis: Looking beyond the lumen with MRI. Stroke 2005;36:2504–2513.
17. Oikawa M, Ota H, Takaya N, Miller Z, Hatsukami TS, Yuan C. Carotid Magnetic Resonance Imaging - A Window to Study Atherosclerosis and Identify High-Risk Plaques. Circ J 2009;73:1765–1773.
18. Young VE, Patterson AJ, Tunnicliffe EM, et al. Signal-to-noise ratio increase in carotid atheroma MRI: a comparison of 1.5 and 3 T. Br J Radiology 2012;85:937–944.
19. Underhill H, Yarnykh VL, Hatsukami TS, et al. Carotid plaque morphology and composition: initial comparison between 1.5 and 3.0 Tesla magnetic field strengths. Radiology 2008;248:550–560.

20. Kerwin WS, Liu F, Yarnykh V, et al. Signal Features of the Atherosclerotic Plaque at 3.0 Tesla Versus 1.5 Tesla: Impact on Automatic Classification. J Magn Reson Imag 2008;28:987–995.
21. Yarnykh VL, Terashima M, Hayes CE, et al. Multicontrast black-blood MRI of carotid arteries: Comparison between 1.5 and 3 Tesla magnetic field strengths. J Magn Reson Imag 2006;23:691-698.
22. Gao T, Zhang Z, Yu W, Zhang Z, Wang Y. Atherosclerotic Carotid Vulnerable Plaque and Subsequent Stroke: A High-Resolution MRI Study. Cerebrovasc Dis 2009;27:345-352.
23. Cai JM, Hatsukami TS, Ferguson MS, et al. In Vivo Quantitative Measurement of Intact Fibrous Cap and Lipid-Rich Necrotic Core Size in Atherosclerotic Carotid Plaque: Comparison of High-Resolution Contrast-Enhanced Magnetic Resonance Imaging and Histology. Circulation 2005;112:3437-3444.
24. Chu BC, Kampschulte A, Ferguson MS, et al. Hemorrhage in the Atherosclerotic Carotid Plaque: A High-Resolution MRI Study. Stroke 2004;35:1097-1084.
25. Takaya N, Yuan C, Chu B, et al. Presence of Intraplaque Hemorrhage stimulates Progression of Carotid Atherosclerotic Plaques: A High-Resolution Magnetic Resonance imaging Study. Circulation 2005;111:2768-2775.
26. Trivedi RA, U-King-Im J, Graves MJ, et al. Multi-sequence In vivo MRI can Quantify Fibrous Cap and Lipid Core Components in Human Carotid Atherosclerotic Plaques. Eur J Vasc Endovasc Surg 2004;28:207-213.
27. Wasserman BA, Smith WI, Trout HH, Cannon RO, Balaban RS, Aral AE. Carotid Artery Atherosclerosis: In Vivo Morphologic Characterization with Gadolinium-enhanced Double-oblique MR Imaging—Initial Results. Radiology 2002;223:566-573.
28. Yuan C, Beach KW, Smith LH Jr, Hatsukami TS. Measurement of Atherosclerotic Carotid Plaque Size In Vivo Using High Resolution Magnetic Resonance Imaging. Circulation 1998;98:2666-2671.

29. Clarke SE, Beletsky V, Hammond RR, Hegele RA and Rutt BK. Validation of Automatically Classified Magnetic Resonance Images for Carotid Plaque Compositional Analysis. Stroke 2006;37:93-97.
30. Cappendijk VC, Cleutjens KBJM, Heeneman S, et al. In vivo detection of hemorrhage in human atherosclerotic plaques with Magnetic Resonance Imaging. J Magn Reson Imag 2004;20:105-110.
31. Cappendijk VC, Heeneman S, Kessels AGH, et al. Comparison of single-sequence T1w TFE MRI with multisequense MRI for the Quantification of lipid-rich necrotic core in atherosclerotic plaque. J Magn Reson Imag 2008;27:1347-1355.
32. Bland JM, Altman DG. Statistical method for assessing agreement between two methods of clinical measurement. Lancet 1986;1:307-310.
33. Liu F, Xu D, Ferguson MS, et al. Automated In Vivo Segmentation of Carotid Plaque MRI with Morphology-Enhanced Probability Maps. Magn Reson Med 2006,55:659–668.
34. Gao T, He X, Yu W, Zhang Z, Wang Y. Atherosclerotic plaque pathohistology and classification with high-resolution MRI. Neurol Res 2011;33:325-330.
35. Saam T, Hetterich H, Hoffmann V et al. Meta-Analysis and Systematic Review of the Predictive Value of Carotid Plaque Hemorrhage on Cerebrovascular Events by Magnetic Resonance Imaging. J Am Coll of Cardiol 2013; 62:1081-1091.
36. van den Bouwhuijsen QJA, Bos D, Ikram MA et al. Coexistence of Calcification, Intraplaque Hemorrhage and Lipid Core within the Asymptomatic Atherosclerotic Carotid Plaque: The Rotterdam Study Cerebrovascular Diseases. 2015 39:319-324.
37. Dobrin PB. Effect of histological preparation on the cross-sectional area of arterial rings. J Surg Res 1996;61:413-415.
38. Eubank WB, Yuan C, Fisher ER, et al. Endarterectomy plaque shrinkage: comparison of T2-weighted MR imaging of ex vivo specimens to histologically processed specimens. J Vasc Invest 1998;4:161–170.

39. Jahnke C, Dietrich T, Paetsch I, et al. Experimental evaluation of the detectability of submillimeter atherosclerotic lesions in ex vivo human iliac arteries with ultrahigh-field (7.0 T) magnetic resonance imaging. Int J Cardiovasc Imaging 2007;23:519–527.
40. Yuan C, Beach KW, Smith LH, Hatsukami TS. Measurement of Atherosclerotic Carotid Plaque Size In Vivo Using High Resolution Magnetic Resonance Imaging. Circulation 1998;98:2666-2671.
41. Constable RT, Gore JC. The loss of small objects in variable TE imaging: implications for FSE, RARE and EPI. Magn Reson Med 1992;28:9-24.
42. Speck O, Weigel M, Scheffler K. Contrast, Mechanisms and Sequences. In: Henning J and Speck O Ed. High-Field MR Imaging. Springer Science & Business Media 2011:81-126.

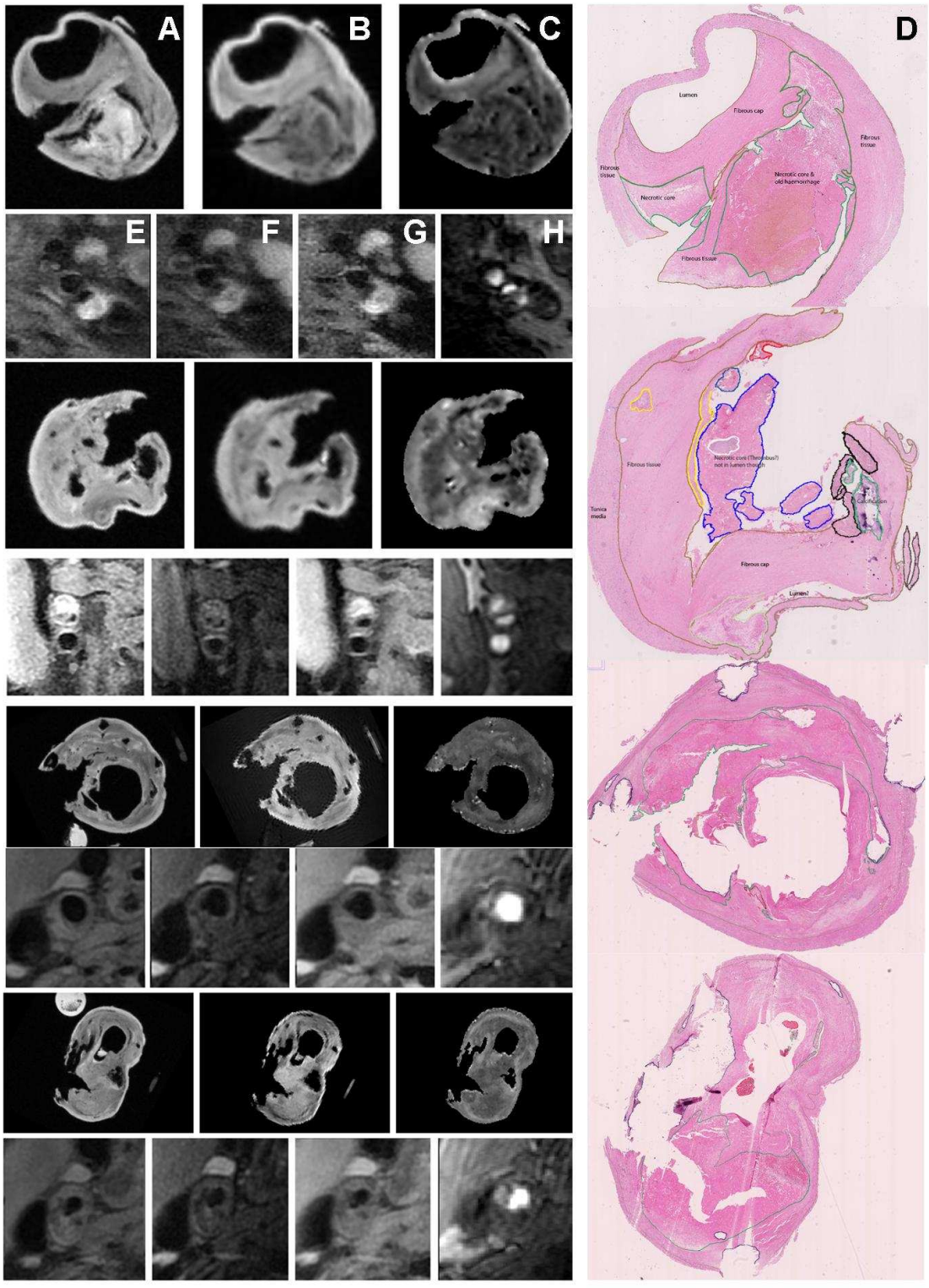


*Figure 1. MR multicontrast weighted images of vulnerable plaque were obtained at 7T ex vivo (A-C) and at 3T in vivo (E-H). Histological images stained with haematoxylin & eosin digitised in D. A and E: T1-w, B and F: T2-w, C: DWI, H: PD-w.*

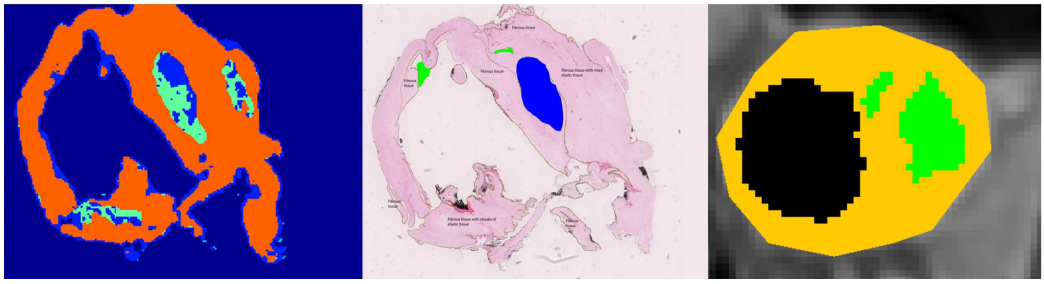

*Figure 2. Segmentation of the 7T (left), Histology (middle) and 3T (right) MR images. 7T MR images were segmented using the relative to the normalised phantom signal intensity and the criterion described in table 1. 3T MR images were segmented using Saam's criterion[15] with signal intensities relative to the sternocleidomastoid muscle. Histology sections were segmented manually. Orange/Yellow = Fibrous tissue, Green = LR/NC with haemorrhage and blue = LR/NC without haemorrhage.*

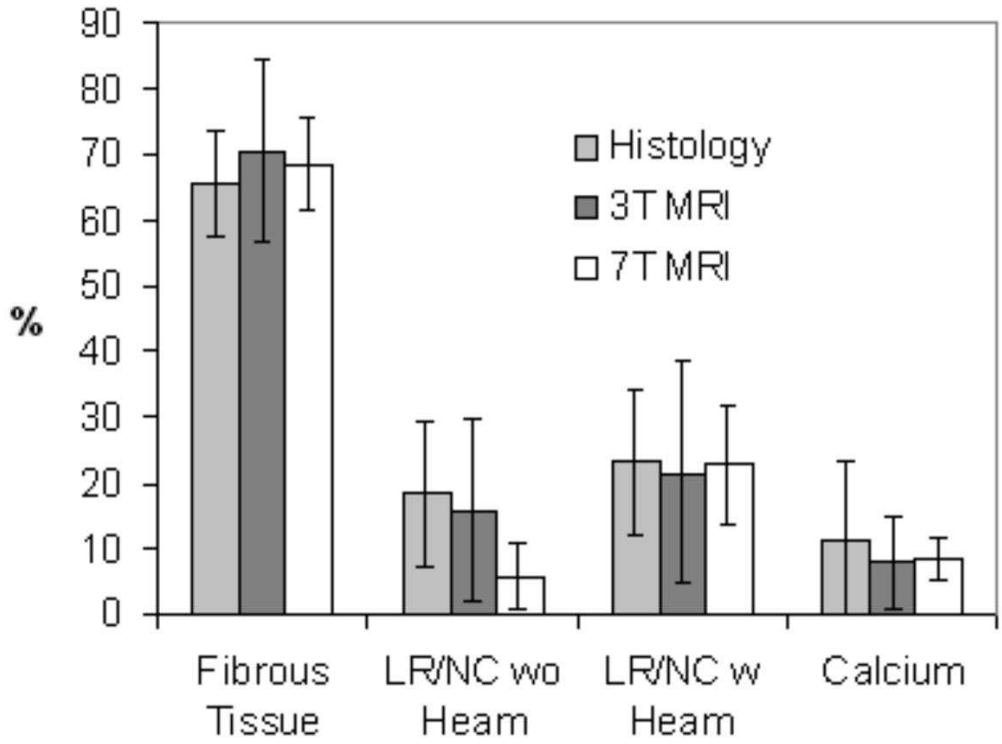


*Figure 3. Plaque composition in percentage of total plaque area of the 3T MRI, 7T MRI and the histology dataset, per artery.*

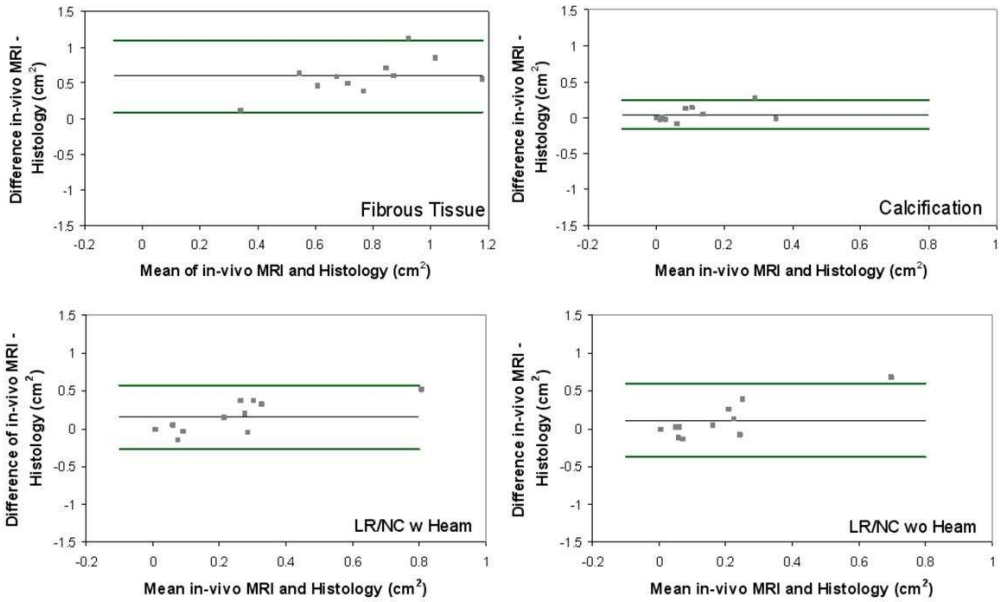


*Figure 4. Bland-Altman plots for the different plaque components of Histology and in-vivo 3T MRI in $cm^2$. These results show a consistently overestimation of the plaque components using 3T MRI.*

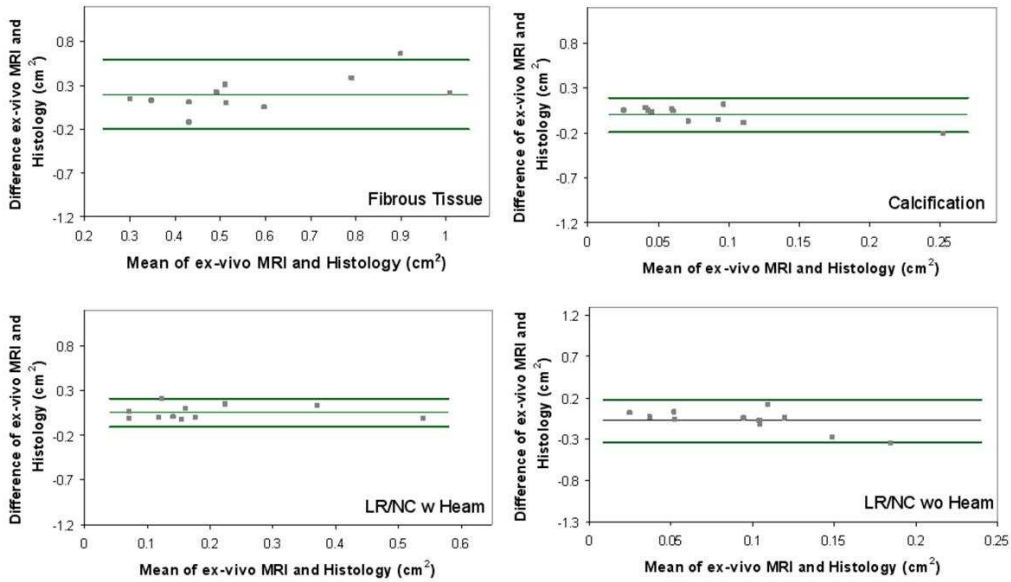


*Figure 5. Bland-Altman plots for different plaque components of Histology and ex-vivo 7T MRI in $cm^2$. These results show a consistently overestimation of the plaque components using 7T MRI.*